J Water Environ Nanotechnol 2026, 11(4): 477-490
10.22090/jwent.2026.2071245.1964

RESEARCH PAPER

Sustainable Synthesis and Multifunctional Applications of Cobalt Chromite Nanoparticles in Wastewater Treatment and Biomedicine

Sonali Dichayal, Rajeshwari Oza*

Department of Chemistry, SN Arts, DJ Malpani and BN Science Sarda College, Sangamner, 422608, India

*Corresponding Author. Email: rajeshwariksaraswat@gmail.com

Article History:

Received: 2025-09-09

Revised: 2026-02-06

Accepted: 2026-02-20

How to cite this article
Dichayal S, Oza R. Sustainable Synthesis and Multifunctional Applications of Cobalt Chromite Nanoparticles in Wastewater Treatment and Biomedicine. J Water Environ Nanotechnol 2026, 11(4): 477-490, DOI: 10.22090/jwent.2026.2071245.1964

HIGHLIGHTS

- First report on the Creation of $CoCr_2O_4$ NPs using cow urine as a reducing and capping agent, eliminating the need for toxic chemicals.
- Under visible light exposure, $CoCr_2O_4$ nanoparticles demonstrated efficient photocatalytic activity, degrading 86.0% of the tetracycline antibiotic within 150 minutes.
- · Demonstrates significant cytotoxic effects against cancer cell lines (e.g., MCF-7), highlighting their potential in cancer therapy.

ABSTRACT

This study reports an environmentally benign and sustainable synthesis of cobalt chromite ($CoCr_2O_4$) nanoparticles employing cow urine as a green precursor and systematically investigates their anticancer and photocatalytic properties. X-ray diffraction (XRD) analysis confirmed the formation of a well-crystallized cubic spinel phase with an average crystallite size of 34.59 nm. Morphological characterization using FESEM and HR-TEM revealed uniformly distributed nanoparticles with a well-defined cubic morphology. UV–visible diffuse reflectance spectroscopy (UV–DRS) demonstrated a narrow optical bandgap of 1.9 eV, indicating strong visible-light absorption capability. The cytotoxic potential of the synthesized $CoCr_2O_4$ nanoparticles was evaluated against human breast cancer (MCF-7) cells, resulting in an IC_{50} value of 286.6 µg/mL, suggesting moderate anticancer activity. Additionally, the photocatalytic performance under visible-light irradiation from a tungsten lamp exhibited excellent efficiency, achieving 86.0% degradation of tetracycline (TC) within 150 min. Overall, these results highlight the potential of green-synthesized $CoCr_2O_4$ nanoparticles as multifunctional materials for environmental remediation and biomedical applications.

KEYWORDS: *Green synthesis, Cobalt Chromite Nanoparticles, Cow urine, Anticancer activity, Photocatalysis*

©2026 The Author(s). Published by the Iranian Environmental Mutagen Society. This work is licensed under the Creative Commons Attribution 4.0 International License (CC BY 4.0). To view a copy of this license, visit http://creativecommons.org/licenses/by/4.0/.

1 INTRODUCTION

The growing need for sustainable, environmentally friendly nanomaterial synthesis techniques has driven research toward green chemistry approaches [1], [2]. Conventional physical and chemical techniques for creating nanoparticles often use hazardous reducing agents, consume high energy, and produce hazardous byproducts, raising environmental and health concerns [3], [4].On the other hand, green synthesis offers a less expensive and environmentally friendly substitute by using natural extracts, bio-wastes, or biological fluids as reducing, capping, and stabilizing agents[5][6], [7], [8].

Cow urine, a readily available bio-waste, has gained attention in green synthesis due to its rich composition of organic compounds, enzymes, and minerals[9]. The biomolecules present in cow urine act as reducing agents that facilitate nanoparticle formation [10]. Its potential for creating metal and metal oxide nanoparticles with improved biological and catalytic capabilities has been shown in recent research [9, 10]. Using cow urine, Santosh et al. synthesized silver nanoparticles and examined their antibacterial and biocompatible qualities. [11] Using cow urine, Dhabhane et al. described the biosynthesis of ZnO NPs and investigated their photocatalytic and medicinal uses [12]. Using cow urine, Ghotekar et al. reported the green production of $BIVO_4$ NPs and investigated their biological and photocatalytic uses [13].

The antibiotic tetracycline is used in both human and veterinary medicine. Tetracycline's extensive usage has caused it to accumulate in water bodies, which has an immediate impact on both the environment and people. [11], [12]. Conventional wastewater treatment approaches, such as membrane filtration, adsorption, and biological therapy, frequently fall short in fully degrading pollutants, highlighting the need for advanced photocatalytic degradation techniques[13], [14]. Spinel-structured nanoparticles, such as $CoCr_2O_4$, demonstrate outstanding photocatalytic performance under visible light irradiation, positioning them as promising materials for the degradation of antibiotics[15]

Additionally, cancer continues to be a major global cause of death, necessitating the creation of innovative treatment medicines with few adverse effects. [16], [17]. Spinel structure metal oxide nanoparticles have shown promising anticancer properties by inducing oxidative stress and apoptosis in cancer cells. [18], [19]. Several studies have documented their efficacy, including Ajith et al., who demonstrated the antibacterial, photocatalytic, and anticancer properties of spinel metal oxides [20]. In another study, Ajith et al. highlighted the photocatalytic, antibacterial, and anticancer activity of nickel chromite [21]. While Ashok et al. reported the anticancer potential of $ZnFe_2O_4$ nanoparticles[22]. Despite these advancements, the anticancer potential of green-synthesized $CoCr_2O_4$ nanoparticles remains largely unexplored [23], [24].

In this work, we present an environmentally friendly creation of $CoCr_2O_4$ NPs with the use of cow urine as a bio-reducing agent. Their photocatalytic efficacy was assessed through the breakdown of tetracycline under visible light exposure. Furthermore, the anticancer potential was assessed against human cancer cell lines, demonstrating their dual functionality in environmental remediation and biomedical applications. This work highlights the sustainable synthesis of $CoCr_2O_4$ nanoparticles and their potential in addressing critical challenges in wastewater treatment and cancer therapy.

2 MATERIALS AND METHODS

2.1 Materials

Cobalt nitrate hexahydrate [$(Co(NO_3)_2.6H_2O$, 98%], chromium nitrate nonahydrate [$(CrNO_3)_3.9H_2O$, 98%], EDTA, Isopropyl alcohol (IPA), benzoquinone, and tetracycline were purchased from Chemo Equip Corporation, Maharashtra, India. Fresh cow urine of the desi cow was collected from Ashvi Village, Sanganer. Cow urine was filtered and kept for later use.

2.2 Green synthesis of $CoCr_2O_4$ NPs

Cobalt chromite nanoparticles were produced using the sol-gel auto-combustion method, with cow urine as a reducing agent. For synthesis, 30 mL of distilled water was used to dissolve a 1:2 M mixture of cobalt nitrate hexahydrate and chromium nitrate nonahydrate, which was then agitated to create a homogeneous, clear solution. [25]. Subsequently, 170 mL of cow urine was added to form a homogeneous paste. The paste was then heated at 70-80°C to form a thick gel. To facilitate auto-combustion, the gel underwent an additional heating step at 170-180°C for 4 h.[26] The subsequent solid was washed 3-4 times with pure water, ethanol, and dilute HCl, & then dried in a desiccator. To enhance its crystalline structure, the product was annealed at 800°C for 4 h.[25]

2.3 Characterizations

The crystalline characteristics of the prepared NPs were examined using X-ray diffraction spectroscopy, with a Bruker D8 single-crystal diffractometer. Fourier Transform Infrared Spectroscopy (FT-IR, Shimadzu, Japan) was used to find out the IR frequencies of the various functional groups in the produced samples. UV-DRS spectrum was noted with a Systronic UV-Vis spectrophotometer. Morphological & elemental analyses were conducted using a Nova NanoSEM 303 field-emission scanning electron microscopy with energy dispersive Spectroscopy (FESEM-EDS) and a high-resolution electron microscopy (HRTEM; JEOL JEM 2100).

2.4 Anticancer Activity-

The anticancer potential of environmentally friendly $CoCr_2O_4$ Nps was assessed using the MTT assay against MCF-7 breast cancer cells. First, the cells were grown for 24 hr at 37^0 C in a humid atmosphere on a customized 96-well plate at a rate of 10000 cells per well. The cells were then mixed with $CoCr_2O_4$

J Water Environ Nanotechnol, 2026, 11(4): 477-490
10.22090/jwent.2026.2071245.1964

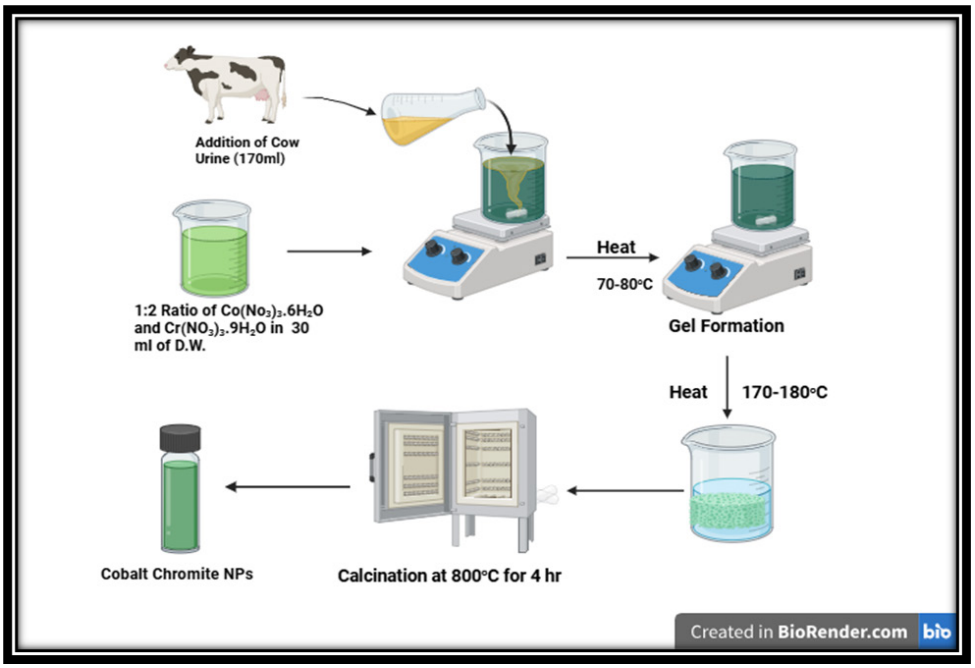


Fig. 1: Representation of the biosynthesis of $CoCr_2O_4$ nanoparticles

NPs at concentrations ranging from 1-1000 µg/mL for 24 hours. A 100 µL stock solution of MTT was added to each well of the plates once the cells were fully mixed, and the plates were then incubated for an extra 4 hours. The solution in the well plate was removed and examined using a microplate reader set to 550 nm once the incubation period was over. Additionally, control cells were used under the same conditions and served as a reference. [27]The solvent used in the sample solution determines the maximum absorbance, and the percentage of viable cells was determined with the help of the formulas below.

% cell viability = A_{550} of treated sample/A_{550} of control* 100

2.5 Photocatalytic study

Photocatalytic degradation of tetracycline (TC) using bio-fabricated $CoCr_2O_4$ nanoparticles (NPs) was evaluated under visible light irradiation from a tungsten lamp. To achieve adsorption-desorption equilibrium, 30 mg of the catalyst was added to 50 mL of TC aqueous solution (10 ppm) and magnetically agitated for 30 minutes in the dark. At specified intervals, aliquots (3 mL) were taken, and the catalyst was extracted by centrifugation. A UV-VIS spectrophotometer was used to measure the absorbance of the solution at λ = 357 nm to track the residual TC content. The adsorption efficiency and photocatalytic degradation performance were calculated based on the decrease in absorbance.[28], [29]

3. RESULTS AND DISCUSSION

3.1 XRD Analysis

X-ray diffraction spectroscopy (XRD) was used to analyze the crystal structure of the produced $CoCr_2O_4$. Fig. 2 displays the XRD pattern of the sample, where all the observed diffraction peaks correspond to the cubic-shaped spinel structure of $CoCr_2O_4$ (JCPDS card no. 22-1084). The prominent diffraction peaks observed at 2θ values of 18.5°, 30.32°, 35.76°, 37.42°, 43.46°, 53.38°, 57.6°, 63.14°, and 74.88°, were indexed to the (111), (220), (311), (222), (400), (422), (511), (440), and (533) crystal planes, respectively, which are characteristic of the spinel structure. The sharp and well-defined peaks indicate the high crystallinity of the sample.[30].The crystallite size was calculated using Scherrer's equation, and the mean crystallite size of the $CoCr_2O_4$ nanoparticles was determined to be 34.59 nm.

3.2FTIR analysis

The FTIR spectrum of the as-synthesized nanocrystalline $CoCr_2O_4$ (Fig. 3) exhibits distinct bands corresponding to M–O vibrational modes within the spinel lattice. Two different absorption bands were identified: a high-frequency band at 608 cm^{-1}, ascribed to the stretching vibrations of Co–O bonds at tetrahedral sites (A-site), and a low-frequency band at 496 cm^{-1}, corresponding to the Cr–O stretching vibrations at octahedral sites (B-site). Additionally, a sharp peak at 894 cm^{-1} was observed, which is associated with the Co–O stretching mode within the spinel lattice. The presence of these characteristic bands confirms the creation of a pure $CoCr_2O_4$ spinel structure, in agreement with previous reports [30], [31]. The absence of extraneous peaks further shows the high purity of the synthesized nanoparticles

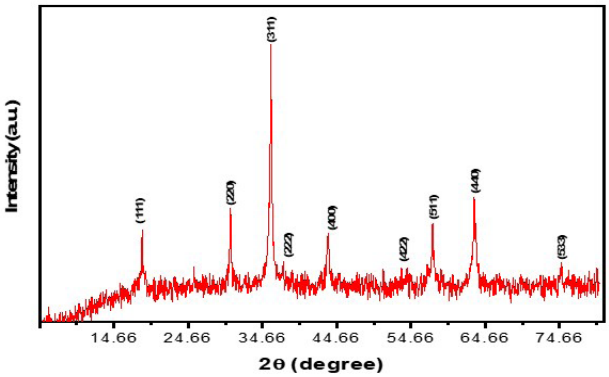


Fig. 2: XRD of biosynthesized $CoCr_2O_4$

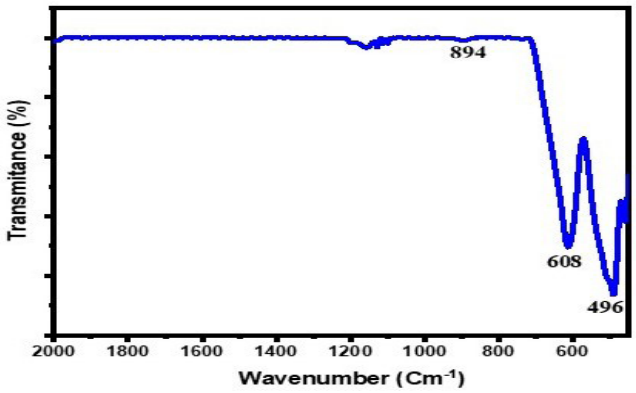


Fig. 3: FTIR Spectra of biosynthesized $CoCr_2O_4$ NPs

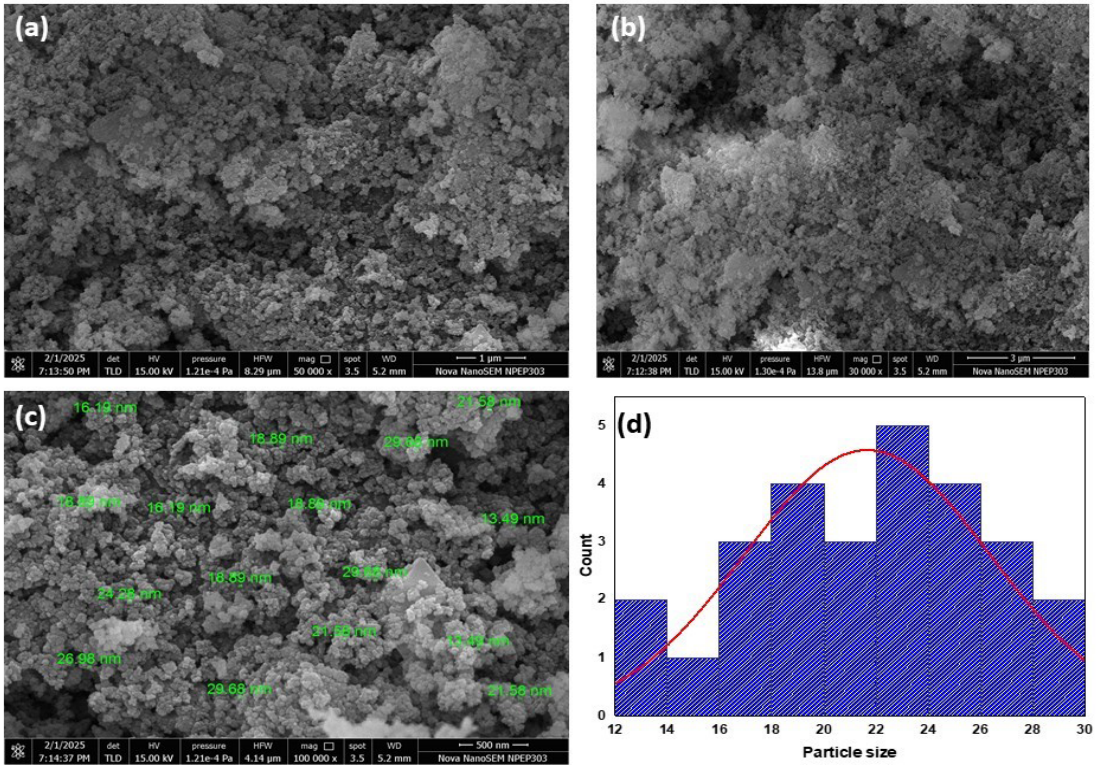


Fig. 4: FESEM images at three diverse magnifications: **(a)** 1 µm, **(b)** 3 µm, and **(c)** 500 nm, and **(d)** particle size distribution of the $CoCr_2O_4$ NPs.

3.4 FESEM and EDX studies

FESEM analysis was carried out to investigate the morphology of the nanoparticles, and the results are shown in Fig. 4. The FESEM images reveal the morphology and size distribution of the synthesized cobalt chromite ($CoCr_2O_4$) nanoparticles. The nanoparticles are uniformly distributed and form interconnected clusters, exhibiting spherical to slightly irregular shapes, which are characteristic of polycrystalline materials.[25] Particle size analysis (Fig. 4d) indicates excellent monodispersity, with an average diameter of 24 nm and a predominant size range of 20-30 nm.

FESEM-EDS were employed to illustrate the composition and morphology of the synthesized $CoCr_2O_4$ nanoparticles. The EDX spectrum (Fig. 5a) clearly shows characteristic peaks corresponding to cobalt (Co), chromium (Cr), and oxygen (O), with no detectable impurities, confirming the phase

J Water Environ Nanotechnol, 2026, 11(4): 477-490
10.22090/jwent.2026.2071245.1964

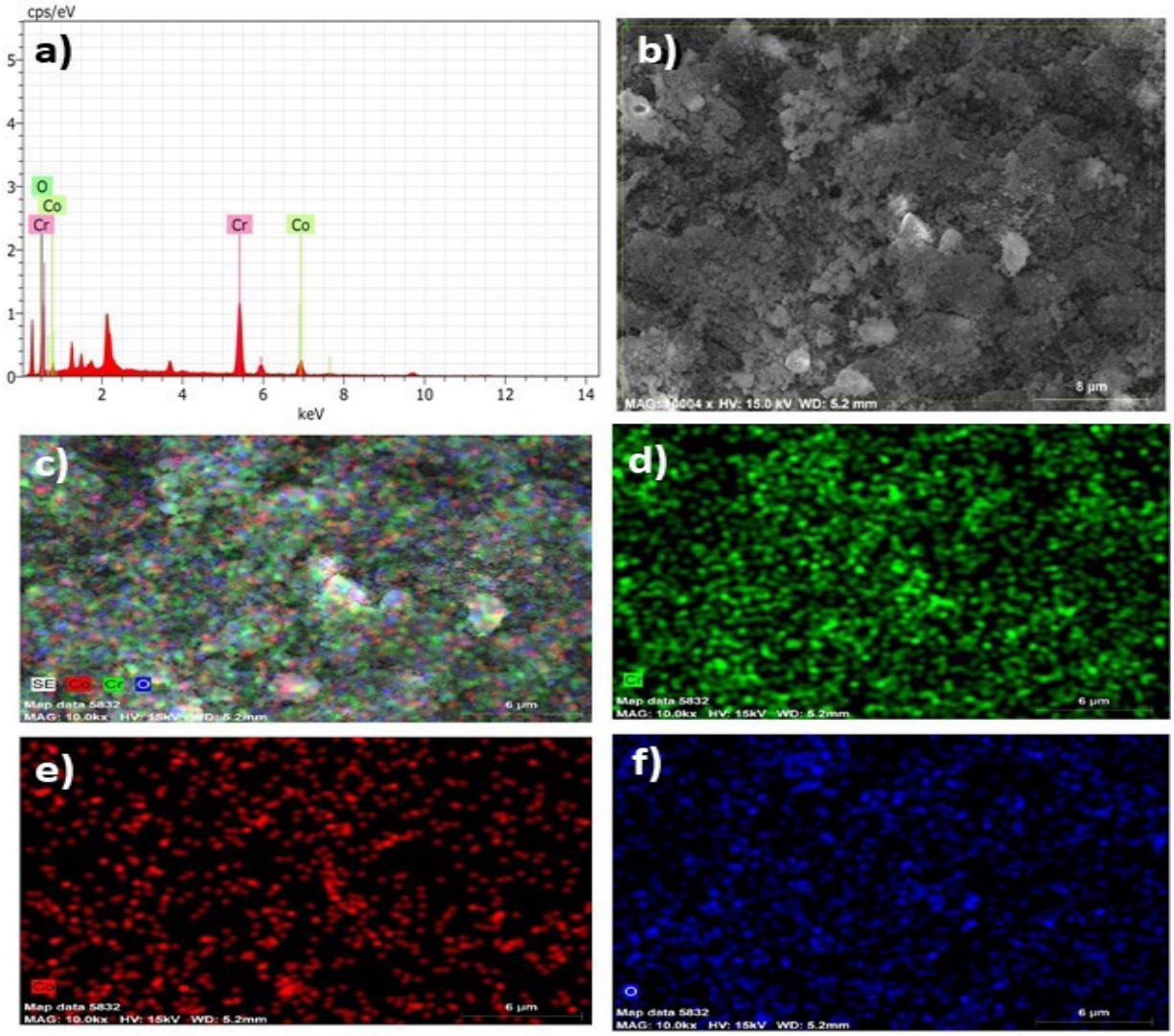


Fig. 5: EDS spectrum of $CoCr_2O_4$ **(a)**, FESEM image of scanned region **(b)**, and elemental mapping spectra (c-f) of $CoCr_2O_4$ nanoparticles.

purity of the material. Elemental mapping analysis (Fig. 5c-f) demonstrates a homogeneous distribution of all constituent elements throughout the sample. These combined results verify the successful synthesis of stoichiometric $CoCr_2O_4$ with both the desired chemical composition and uniform microstructure.

3.5 HRTEM analysis

High-resolution transmission electron microscopy (HR-TEM) was employed to examine the microstructural features of the synthesized $CoCr_2O_4$ nanoparticles. Figs. 6a and 6b show that the nanoparticles possess a pseudo-spherical morphology. The HR-TEM image in Fig. 6c reveals well-defined lattice fringes with an interplanar spacing of 0.45 nm, indicating the crystalline nature of the nanoparticles. The corresponding selected-area electron diffraction (SAED) pattern (Fig. 6d) exhibits distinct diffraction rings indexed to the (111) plane, confirming the polycrystalline structure of the material. These results collectively confirm the high crystallinity and phase purity of the synthesized $CoCr_2O_4$ nanoparticles[30].

3.6 UV-Vis absorption analysis

The optical properties of $CoCr_2O_4$ nanoparticles were studied using UV-Vis diffuse reflectance spectroscopy (UV-DRS). As shown in Fig. 7a, the absorption spectrum exhibits distinct absorption bands in the UV and visible regions, confirming their broad-spectrum light absorption capability. Tauc plot analysis (Fig. 7b) demonstrated a direct bandgap of 1.9 eV, consistent with the observed visible-light absorption properties. The narrow bandgap energy suggests these biosynthesized $CoCr_2O_4$ NPs exhibit excellent potential for

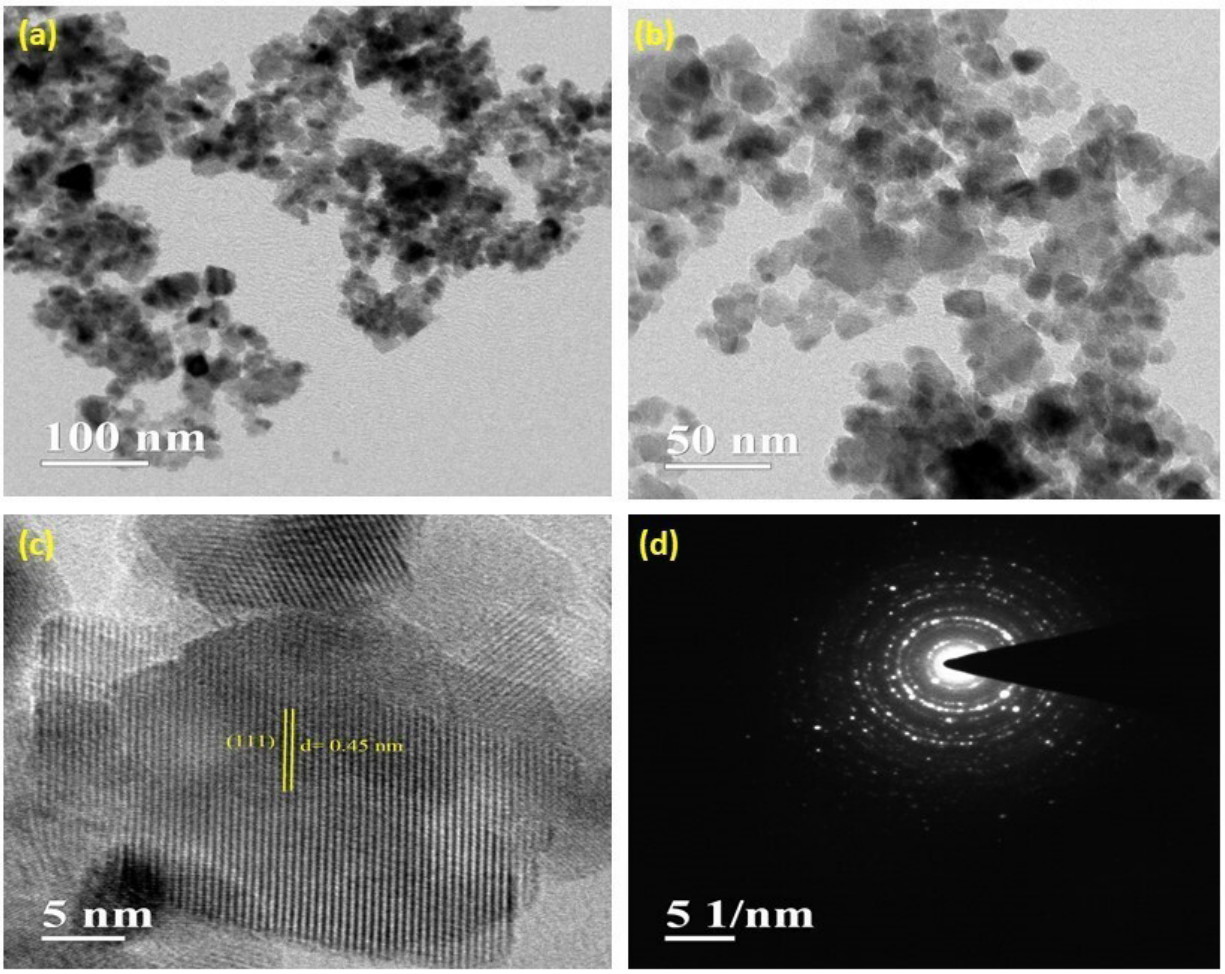


Fig. 6 TEM images of $CoCr_2O_4$ at different resolutions: a)100 nm, b) 50 nm, c) HRTEM image shows lattice plane with d-spacing 0.45 nm, d) SAED pattern

visible-light-responsive photocatalytic applications.[32]

3.7 Anticancer studies of $CoCr_2O_4$ NPs by MTT assay

The cytotoxic potential of $CoCr_2O_4$ nanoparticles (NPs) against MCF7 breast cancer cells was evaluated using the MTT assay. [33]Cells were exposed to a concentration gradient of $CoCr_2O_4$ NPs (1–1000 μg/mL) for 24 hours, with untreated cells serving as the control. The results showed that the dose-dependent cytotoxicity, with cell viability progressively decreasing from 93.89% at 1 μg/mL to 16.50% at 1000 μg/mL (Fig. 8). The half-maximal inhibitory concentration (IC_{50}) was determined to be 286.6 μg/mL, representing moderate anticancer activity.

Microscopic images of MCF-7 cells (Figs. 9a–h) reveal distinct morphological changes in response to CoCr2O4 nanoparticle (NP) treatment. As the concentration of CoCr2O4 NPs increases, a corresponding decrease in cell viability is observed, demonstrating their significant anticancer activity[34], [35]. To the best of our knowledge, this study is the first to report the anticancer properties of $CoCr_2O_4$ NPs, demonstrating their potential as a cytotoxic agent against breast cancer cells.

3.8 Photocatalytic studies

3.8.1 Impact of photocatalyst loading

The photocatalytic degradation efficiency of tetracycline was systematically evaluated as a function of catalyst ($CoCr_2O_4$ NPs) dosage, with variations from 10 to 50 mg[36] (Fig.10). A direct correlation was observed between the degradation rate and catalyst loading, with optimal performance achieved at 30 mg, yielding 82 % degradation within 150 minutes under visible light irradiation. This enhancement is attributed to the increased availability of active sites and improved photon absorption at higher catalyst concentrations. However, beyond the optimal dose, degradation efficiency is reduced as the catalyst dose increases. This may be due to light scattering effects and particle

J Water Environ Nanotechnol, 2026, 11(4): 477-490
10.22090/jwent.2026.2071245.1964

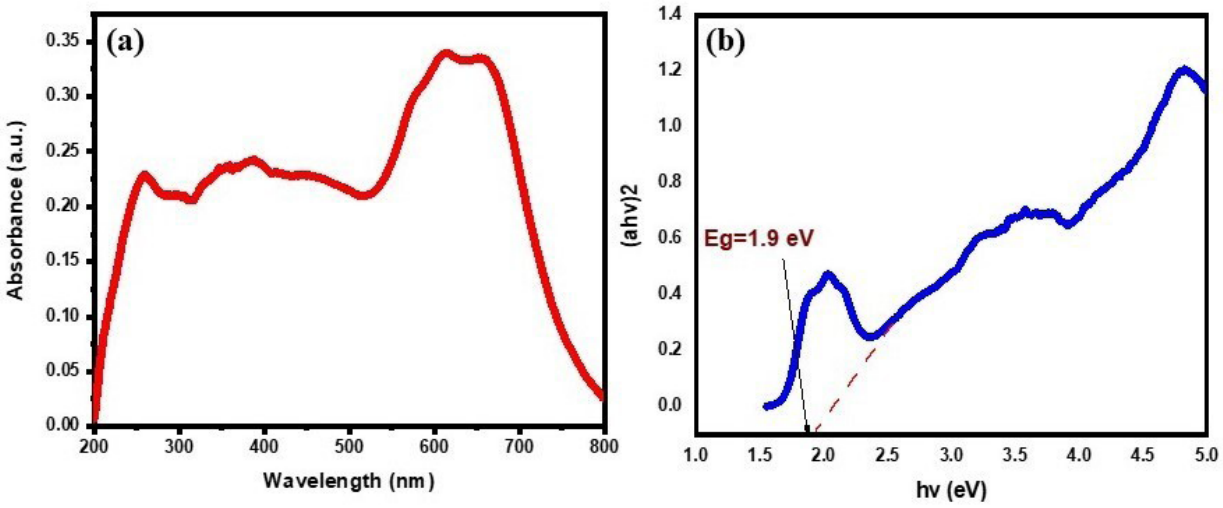


Fig. 7: a) UV-VIS spectra, b) band gap of $CoCr_2O_4$ estimated from Tauc's plot

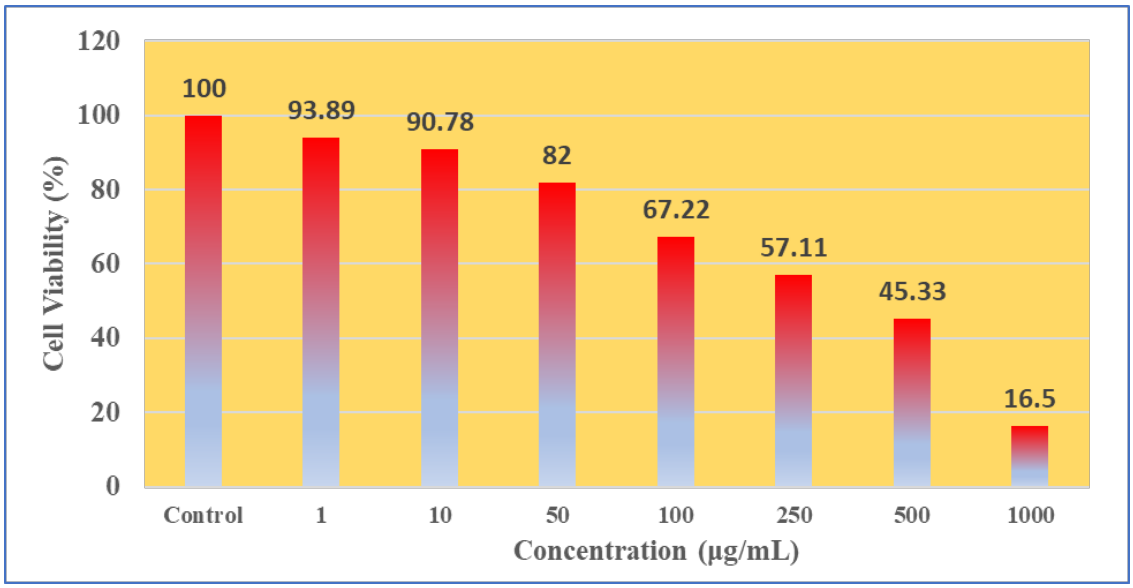


Fig. 8: Anticancer effectiveness of $CoCr_2O_4$ NPs on the MCF-7 cell line

agglomeration, which reduce surface accessibility and hinder light penetration. [37], [38]

3.8.2 Effect of Initial Concentration of Tetracycline

To set the ideal degradation parameter, the concentration of the pollutant plays a very important role. In this study, we systematically evaluated the tetracycline (TC) degradation performance of $CoCr_2O_4$ nanoparticles under visible light irradiation across a concentration range of 10-40 mg/L (Fig. 11). The optimal degradation efficiency (86.05%) was achieved at 20 mg/L TC within 150 min. As TC pollutant concentration increases above 20 mg/L, the degradation efficiency decreases, which may be due to competitive adsorption and light shielding effects. [39], [40]These results demonstrate that while the $CoCr_2O_4$ photocatalyst exhibits effective TC degradation capability, its performance is significantly influenced by the initial pollutant concentration, with optimal efficiency observed at moderate TC concentrations.

3.8.3 Effect of irradiation time

The photodegradation efficiency of biosynthesized $CoCr_2O_4$ nanoparticles was evaluated using tetracycline (TC) as a model pollutant. UV-Vis spectral analysis (Fig. 12a) revealed two characteristic absorption peaks of TC in the UV (λ max = 275 nm) and near-visible (λ max = 355 nm) regions, which served as monitoring wavelengths for degradation studies. As

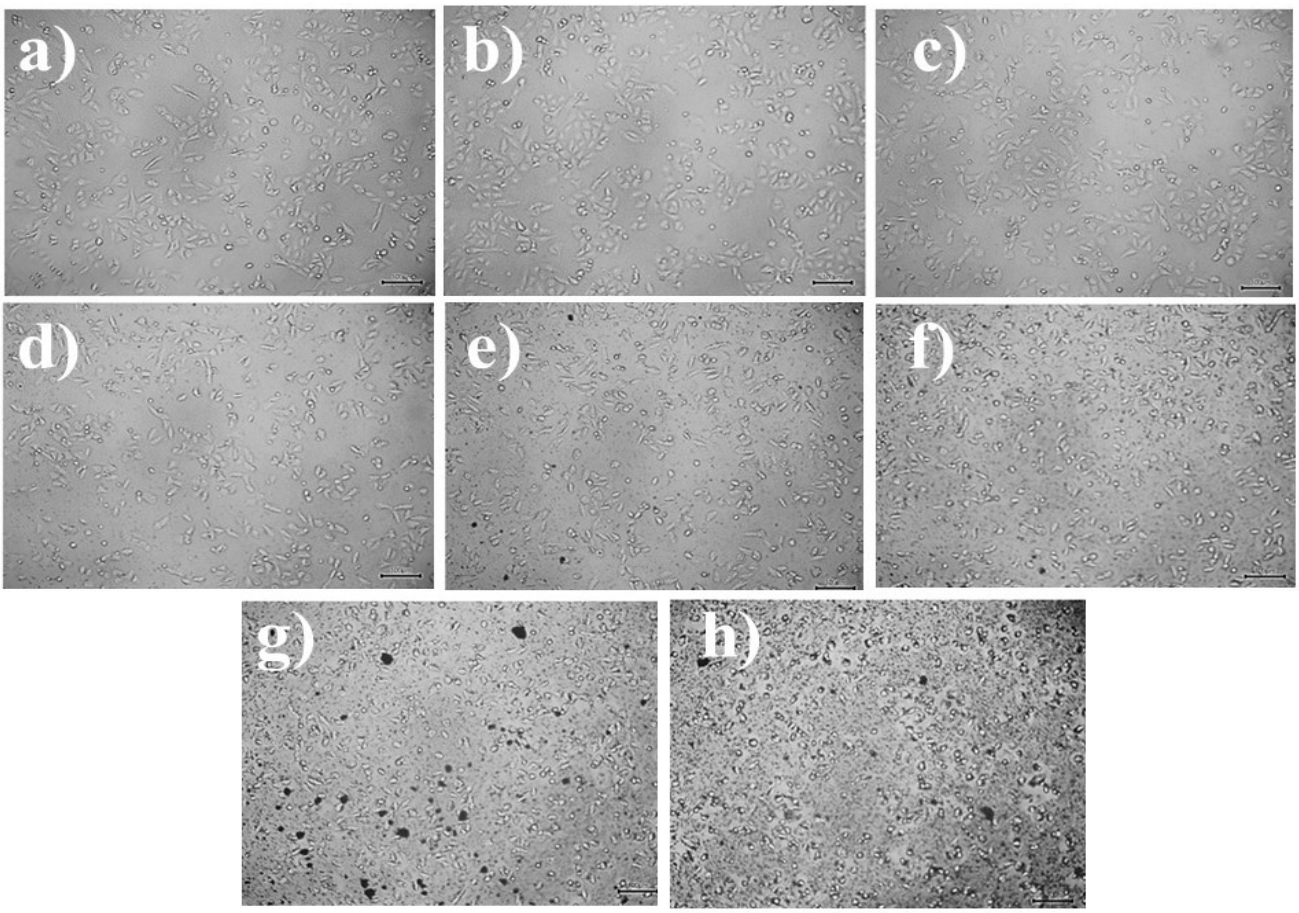


Fig. 9 Morphology of MCF7 cells untreated **(a)**, 1 µg/mL**(b)**,10 µg/mL **(c)**, 50 µg/mL **(d)**, 100 µg/mL**(e)**, 250 µg/mL**(f)**, 500 µg/mL**(g)**, and 1000 µg/mL**(h)**.

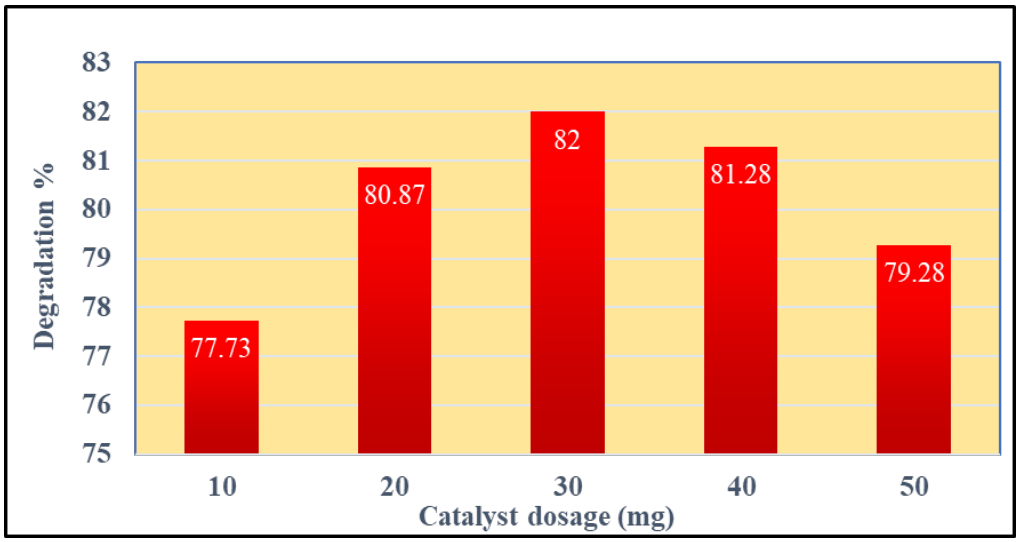


Fig. 10 Effect of catalyst $CoCr_2O_4$ dosage on TC degradation

J Water Environ Nanotechnol, 2026, 11(4): 477-490
10.22090/jwent.2026.2071245.1964

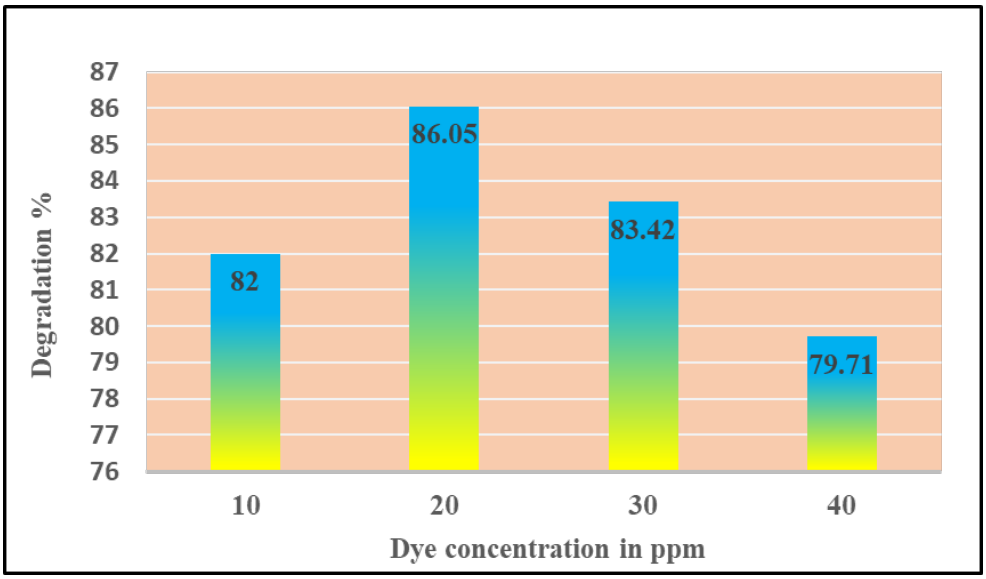


Fig. 11: Effect of TC concentration on the degradation performance using $CoCr_2O_4$ photocatalyst

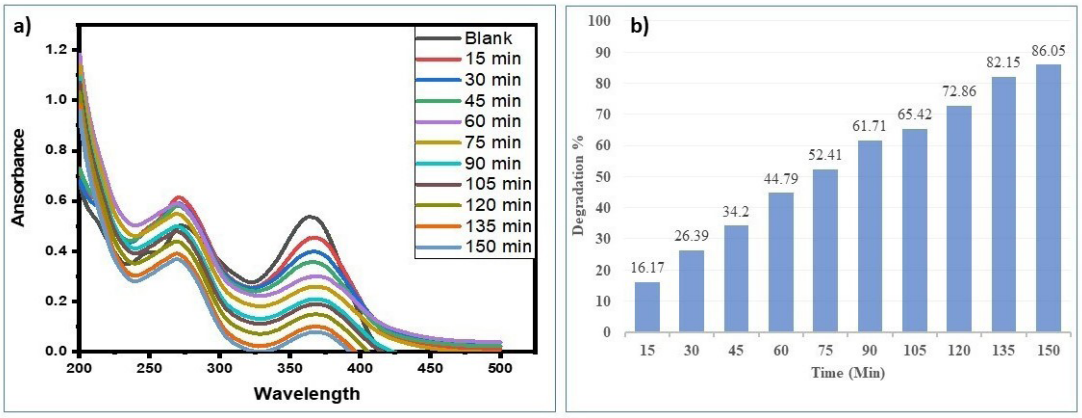


Fig. 12: Photocatalytic degradation of tetracycline using $CoCr_2O_4$ NPs a) Time-dependent UV-VIS absorbance spectra b) time-dependent Degradation

shown in Fig. 12(b), the degradation efficiency increased with irradiation time, reaching a maximum of 86.05% after 150 min. This result shows that degradation efficiency increases with increasing irradiation time. Beyond 150 min. no significant improvement was observed, likely due to the fewer active sites on the nanoparticle surface.[41], [42]

A comparative analysis between the green-synthesized NPs and conventional chromite-based catalysts for TC degradation is presented in the Table. However, literature on TC degradation using biosynthesized nanoparticles remains limited. Future studies should explore the potential of CoCr2O4 NPs to further improve degradation efficiency and reduce environmental pollution.

3.8.5 Scavenging Experiment and possible mechanism for the degradation of tetracycline

The free-radical scavenging experiments were carried out to identify the photogenerated active species involved in the photocatalytic degradation process. Isopropyl alcohol (IPA) was used as a scavenger for hydroxyl radicals (•OH), benzoquinone (BQ) as a scavenger for superoxide radicals ($•O_2^-$), and disodium EDTA (Na_2EDTA) as a hole (h^+) scavenger [47]. [48]. Fig. 13 illustrates the effect of these scavengers on the degradation efficiency of tetracycline (TC).

In the presence of Na_2EDTA, the degradation efficiency decreased slightly from 86.05% to 75.09%, indicating a relatively minor contribution of photogenerated holes. In contrast, the addition of IPA and BQ resulted in a pronounced reduction

Table 1. A comparative analysis of various chromite-based photocatalysts for the degradation of organic pollutants

Catalysts	Organic pollutant	Band gap (eV)	Light	Catalyst dose	Concentration of dye/ antibiotic (ppm)	Time for degradation (min)	Degradation %	Ref.
$CoCr_2O_4$	Malachite green	2.39	Sunlight	25 mg	20	90 min.	91.33	[43]
$CoCr_2O_4$	Congo red	1.74	Solar light	0.2g/l	15	180 min	94	[44]
$CoCr_2O_4$	Eriochrome black T	2.4	Visible light	0.04 g	20	90 min	90	[45]
$CoCr_2O_4$/ BiOBr	Rhodium B and Tetracycline hydrochloride	-	LED light	-	-	15 min 300 min	96 96.7	[46]
$CoCr_2O_4$	Tetracycline	1.9	Visible light	30 mg	20 mg	150 min	86.05	Present work

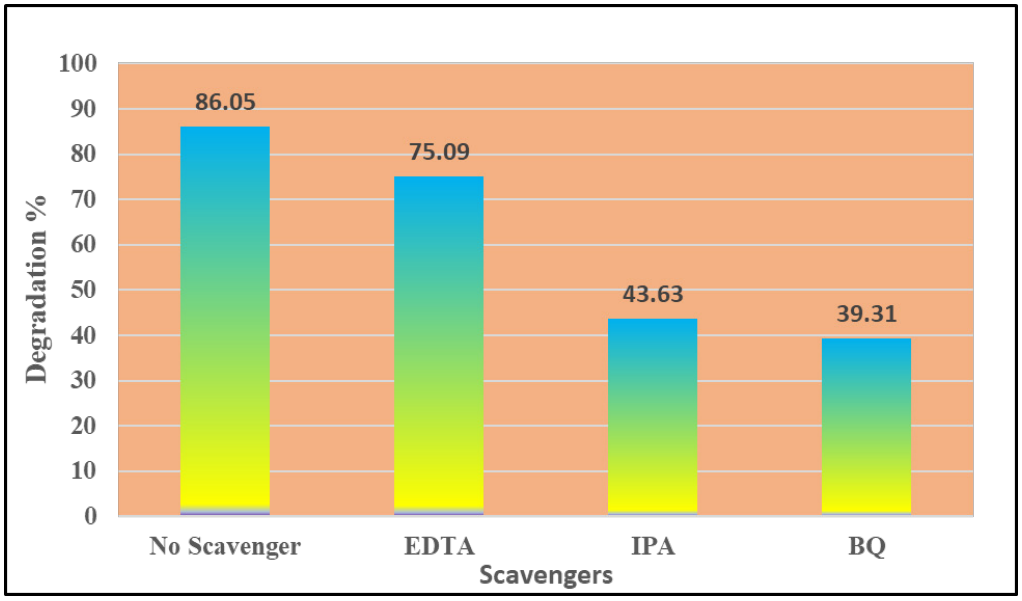


Fig. 13: Impact of various scavengers on the degradation of TC

in degradation efficiency to 43.63% and 39.31%, respectively. These results clearly suggest that hydroxyl radicals (•OH) and superoxide radicals ($•O_2^-$) are the dominant reactive oxygen species responsible for the degradation of tetracycline in the solution.

Based on these observations, a possible photocatalytic degradation mechanism of tetracycline over $CoCr_2O_4$ under visible-light irradiation is proposed. Upon visible-light illumination, $CoCr_2O_4$ absorbs photons and generates electron–hole pairs through the excitation of electrons from the valence band (VB) to the conduction band (CB)[49].

The photogenerated electrons react with dissolved oxygen to produce superoxide radicals ($•O_2^-$), while the holes oxidize surface-adsorbed water or hydroxide ions to form hydroxyl radicals (•OH). These highly reactive oxygen species subsequently attack the tetracycline molecules, leading to the cleavage of complex molecular structures and their conversion into smaller, less harmful intermediates, ultimately resulting in mineralization.[50], [51]. The results of the scavenging experiments strongly support the involvement of •OH and $•O_2^-$ radicals in the photocatalytic degradation process. A schematic illustration of the proposed photocatalytic mechanism is presented in Fig. 14.

3.8.6 Reusability of the photocatalyst

The stability of the synthesized $CoCr_2O_4$ photocatalyst was evaluated through reusability experiments. Reusability tests were performed under optimized conditions, using 50 mL of a 20 ppm tetracycline (TC) solution under visible-light

J Water Environ Nanotechnol, 2026, 11(4): 477-490
10.22090/jwent.2026.2071245.1964

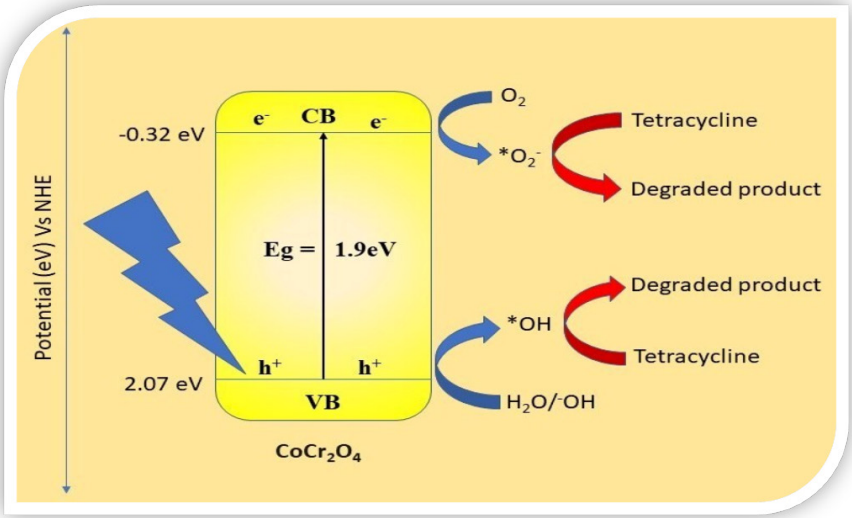


Fig. 14: Degradation mechanism of tetracycline using CoCr2O4 nanoparticles

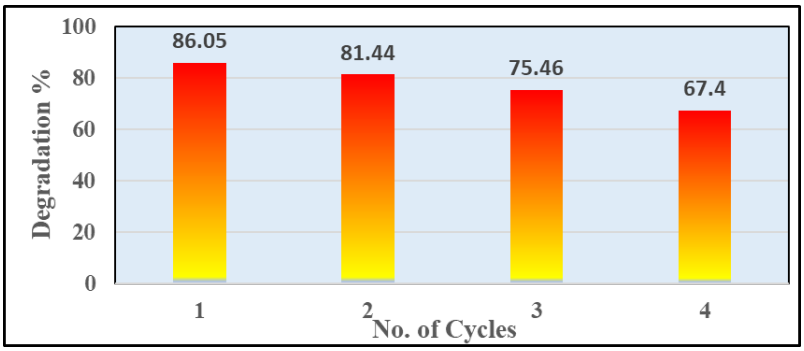


Fig. 15: Reusability study of the $CoCr_2O_4$catalyst

irradiation for 150 min with the ideal photocatalyst dosage. After each photocatalytic cycle, the catalyst was recovered through centrifugation followed by filtration using Whatman filter paper. The collected material was then thoroughly washed with distilled water and ethanol to remove residual contaminants. Finally, the photocatalyst was dried at 110 °C for 2 h to ensure complete solvent removal before reuse in subsequent degradation tests. This procedure was repeated to assess the catalyst's long-term stability and reusability. The photocatalyst exhibited a decomposition performance of 67.40 % in the fourth cycle, as shown in Fig. 15, indicating notable stability for up to four operating cycles. The total degradation analysis confirms that the $CoCr_2O_4$ nanoparticles exhibit high stability as a catalyst for tetracycline degradation. The slight decrease in degradation efficiency observed over multiple cycles may be attributed to a reduction in the active surface area of the catalyst due to partial aggregation or adsorption of residual intermediates [52].

4 CONCLUSION

In this study, $CoCr_2O_4$ nanoparticles (NPs) were successfully synthesized using cow urine as a green and cost-effective fuel, leveraging its organic constituents as natural capping and stabilizing agents. Comprehensive characterization via XRD, FTIR, UV-DRS, FESEM, EDX, and TEM confirmed the formation of well-defined $CoCr_2O_4$ NPs with desirable structural and optical properties. The NPs exhibited significant photocatalytic activity, achieving 86.05% degradation of tetracycline, while maintaining 67% efficiency after four regeneration cycles, demonstrating excellent reusability. Additionally, the NPs displayed promising anticancer activity against MCF-7 breast cancer cells, with an IC_{50} value of 286.6 µg/mL. These findings highlight the dual functionality of $CoCr_2O_4$ NPs in environmental remediation and biomedical applications. The eco-friendly synthesis approach presented here offers a sustainable and scalable alternative for nanoparticle production, with potential for further optimization and

application in diverse fields. Future studies will focus on enhancing photocatalytic efficiency and exploring mechanistic insights into their biological activity.

Declaration of competing interests
The authors state that no known conflicting financial interests or personal relationships could have influenced any of the work reported in this study.

Data availability
Data will be available on reasonable request

Acknowledgment
We are sincerely grateful to the Amrutvahini College of Engineering and Amrutvahini College of Pharmacy, Sangamner, for their support of this work.

Statements and Declarations
The authors declare that no funds, grants, or other support were received during the preparation of this manuscript.

REFERENCES

[1] M. M. Abady, D. M. Mohammed, T. N. Soliman, R. A. Shalaby, and F. A. Sakr, "Sustainable synthesis of nanomaterials using different renewable sources," Bull Natl Res Cent, vol. 49, no. 1, p. 24, Apr. 2025, doi: 10.1186/s42269-025-01316-4. https://doi.org/10.1186/s42269-025-01316-4

[2] S. F. Ahmed et al., "Green approaches in synthesising nanomaterials for environmental nanobioremediation: Technological advancements, applications, benefits and challenges," Environ Res, vol. 204, p. 111967, Mar. 2022, doi: 10.1016/j.envres.2021.111967. https://doi.org/10.1016/j.envres.2021.111967

[3] R. Saxena et al., "A review on green synthesis of nanoparticles toward sustainable environment," Sustainable Chemistry for Climate Action, vol. 6, p. 100071, Jun. 2025, doi: 10.1016/j.scca.2025.100071. https://doi.org/10.1016/j.scca.2025.100071

[4] A. Nyabadza et al., "A review of physical, chemical and biological synthesis methods of bimetallic nanoparticles and applications in sensing, water treatment, biomedicine, catalysis and hydrogen storage," Adv Colloid Interface Sci, vol. 321, p. 103010, Nov. 2023, doi: 10.1016/j.cis.2023.103010. https://doi.org/10.1016/j.cis.2023.103010

[5] V. M. S. D. S. P. D. H. R. O. S. Dichayal, "Green Synthesis of Cobalt Ferrite Nanoparticles: A Comprehensive Review on Eco-friendly Approaches, Characterization Techniques, and Potential Applications," Journal of Chemical Reviews, vol. 6, no. 4, pp. 514-531, 2024.

[6] H. Singh et al., "Revisiting the Green Synthesis of Nanoparticles: Uncovering Influences of Plant Extracts as Reducing Agents for Enhanced Synthesis Efficiency and Its Biomedical Applications," Int J Nanomedicine, vol. Volume 18, pp. 4727-4750, Aug. 2023, doi: 10.2147/IJN.S419369. https://doi.org/10.2147/IJN.S419369

[7] H. M. Abuzeid, C. M. Julien, L. Zhu, and A. M. Hashem, "Green Synthesis of Nanoparticles and Their Energy Storage, Environmental, and Biomedical Applications," Crystals (Basel), vol. 13, no. 11, p. 1576, Nov. 2023, doi: 10.3390/cryst13111576. https://doi.org/10.3390/cryst13111576

[8] S. Shahzadi, S. Fatima, Q. ul ain, Z. Shafiq, and M. R. S. A. Janjua, "A review on green synthesis of silver nanoparticles (SNPs) using plant extracts: a multifaceted approach in photocatalysis, environmental remediation, and biomedicine," RSC Adv, vol. 15, no. 5, pp. 3858-3903, 2025, doi: 10.1039/D4RA07519F. https://doi.org/10.1039/D4RA07519F

[9] S. Dichayal et al., "Synthesis, characterization, and photocatalytic potential of CoFe2O4 nanoparticles immobilized on graphitic carbon nitride," Transition Metal Chemistry, Jul. 2025, doi: 10.1007/s11243-025-00667-1. https://doi.org/10.1007/s11243-025-00667-1

[10] H. Dabhane et al., "Cow urine mediated green synthesis of nanomaterial and their applications: A state-of-the-art review," Journal of Water and Environmental Nanotechnology, vol. 6, no. 1, pp. 81-91, 2021, doi: 10.22090/jwent.2021.01.008.

[11] F. Ahmad, D. Zhu, and J. Sun, "Environmental fate of tetracycline antibiotics: degradation pathway mechanisms, challenges, and perspectives," Environ Sci Eur, vol. 33, no. 1, p. 64, Dec. 2021, doi: 10.1186/s12302-021-00505-y. https://doi.org/10.1186/s12302-021-00505-y

[12] L. Albarano et al., "Assessment of ecological risks posed by veterinary antibiotics in European aquatic environments: A comprehensive review and analysis," Science of The Total Environment, vol. 954, p. 176280, Dec. 2024, doi: 10.1016/J.SCITOTENV.2024.176280. https://doi.org/10.1016/j.scitotenv.2024.176280

[13] S. Mishra and B. Sundaram, "A review of the photocatalysis process used for wastewater treatment," Mater Today Proc, vol. 102, pp. 393-409, Jan. 2024, doi: 10.1016/J.MATPR.2023.07.147. https://doi.org/10.1016/j.matpr.2023.07.147

[14] J. Iyyappan, B. Gaddala, R. Gnanasekaran, M. Gopinath, D. Yuvaraj, and V. Kumar, "Critical review on wastewater treatment using photo catalytic advanced oxidation process: Role of photocatalytic materials, reactor design and kinetics," Case Studies in Chemical and Environmental Engineering, vol. 9, p. 100599, Jun. 2024, doi: 10.1016/J.CSCEE.2023.100599. https://doi.org/10.1016/j.cscee.2023.100599

[15] B. Paul, B. Bhuyan, D. D. Purkayastha, S. S. Dhar, and S. Behera, "Facile synthesis of spinel CuCr2O4 nanoparticles and studies of their photocatalytic activity in degradation of some selected organic dyes," J Alloys Compd, vol. 648, pp. 629-635, Nov. 2015, doi: 10.1016/j.jallcom.2015.07.012. https://doi.org/10.1016/j.jallcom.2015.07.012

[16] D. C. Joshi et al., "Novel therapeutic agents in clinical trials: emerging approaches in cancer therapy," Discover Oncology, vol. 15, no. 1, p. 342, Aug. 2024, doi: 10.1007/s12672-024-01195-7. https://doi.org/10.1007/s12672-024-01195-7

[17] A. Zafar, S. Khatoon, M. J. Khan, J. Abu, and A. Naeem, "Advancements and limitations in traditional anti-cancer therapies: a comprehensive review of surgery, chemotherapy, radiation therapy, and hormonal therapy," Discover Oncology, vol. 16, no. 1, p. 607, Apr. 2025, doi: 10.1007/s12672-025-02198-8. https://doi.org/10.1007/s12672-025-02198-8

[18] J.-J. Xu, W.-C. Zhang, Y.-W. Guo, X.-Y. Chen, and Y.-N. Zhang, "Metal nanoparticles as a promising technology in targeted cancer treatment," Drug Deliv, vol. 29, no. 1, pp. 664-678, Dec. 2022, doi: 10.1080/10717544.2022.2039804. https://doi.org/10.1080/10717544.2022.2039804

[19] J. Sidhic et al., "Advancements in metal and metal oxide nanoparticles for targeted cancer therapy and imaging: Mechanisms, applications, and safety concerns," J Drug Deliv Sci Technol, vol. 105, p. 106622, Mar. 2025, doi: 10.1016/J.JDDST.2025.106622. https://doi.org/10.1016/j.jddst.2025.106622

[20] A. A, T. A. Wani, S. G, and S. N, "A facile synthesis and characterization of spinel Zinc-Chromite (ZnCr2O4) nanoparticles: their photocatalytic, antibacterial, and anticancer activities," J Solgel Sci Technol, vol. 110, no. 1, pp. 74-89, Apr. 2024, doi: 10.1007/s10971-024-06346-4. https://doi.org/10.1007/s10971-024-06346-4

[21] A. Ajith, T. A. Wani, G. Suresh, N. Saravanan, and R. Masrour, "Sol-Gel Synthesis and Characterizations of Spinel Nickel Chromite (NiCr 2 O 4) Nanoparticles to Study their Photocatalytic, Antibacterial and Anticancer Activities," Nano, vol. 19, no. 09, Aug. 2024, doi: 10.1142/S1793292024500504. https://doi.org/10.1142/S1793292024500504

[22] K. Ashok, P. Usha, N. R., T. Ramesh, N. P. Kumar, and G. M. Sulaiman, "Multifunctional Characterization and Anticancer Properties of Magnetic Zinc Ferrite Nanoparticles by Modified Ultrasonic Assisted Co-precipitation Method," ECS Journal of Solid State Science and Technology, vol. 13, no. 8, p. 083011, Aug. 2024, doi: 10.1149/2162-8777/ad71f2. https://doi.org/10.1149/2162-8777/ad71f2

[23] S. Sargazi et al., "Application of Green Gold Nanoparticles in Cancer Therapy and Diagnosis," Nanomaterials, vol. 12, no. 7, p. 1102, Mar. 2022, doi: 10.3390/nano12071102. https://doi.org/10.3390/nano12071102

[24] E. Tinajero-Díaz et al., "Green Metallic Nanoparticles for Cancer Therapy: Evaluation Models and Cancer Applications," Pharmaceutics, vol. 13, no. 10, p. 1719, Oct. 2021, doi: 10.3390/pharmaceutics13101719. https://doi.org/10.3390/pharmaceutics13101719

[25] K. Patel et al., "Insights into the solar-light-driven photocatalysis of greenly synthesized CoCr2O4 nanoparticles using Azadirachta indica," J Solgel Sci Technol, vol. 114, no. 2, pp. 594-611, May 2025, doi: 10.1007/s10971-025-06711-x. https://doi.org/10.1007/s10971-025-06711-x

[26] S. P. V.-H. N. S. B. K.-Y. A. L. H. C. A. M. & R. O. Suresh Ghotekar, "Spinel ZnCr2O4 nanorods synthesized by facile sol-gel auto combustion method with biomedical properties," Journal of Sol-Gel Science and Technology, vol. 105, p. 176181765, Nov. 2023. https://doi.org/10.1007/s10971-022-05964-0

[27] A. Ali et al., "Ligand substituent effect on the cytotoxicity activity of two new copper(<scp>ii</scp>) complexes bearing 8-hydroxyquinoline derivatives: validated by MTT assay and apoptosis in MCF-7 cancer cell line (human breast cancer)," RSC Adv, vol. 11, no. 24, pp. 14362-14373, 2021, doi: 10.1039/D1RA00172H. https://doi.org/10.1039/D1RA00172H

[28] K. Song et al., "Efficient tetracycline degradation under visible light irradiation using CuBi2O4/ZnFe2O4 type II heterojunction photocatalyst based on two spinel oxides," J Photochem Photobiol A Chem, vol. 433, p. 114122, Dec. 2022, doi: 10.1016/j.jphotochem.2022.114122. https://doi.org/10.1016/j.jphotochem.2022.114122

[29] S. Liu, A. Zada, X. Yu, F. Liu, and G. Jin, "NiFe2O4/g-C3N4 heterostructure with an enhanced ability for photocatalytic degradation of tetracycline hydrochloride and antibacterial performance," Chemosphere, vol. 307, p. 135717, Nov. 2022, doi: 10.1016/j.chemosphere.2022.135717. https://doi.org/10.1016/j.chemosphere.2022.135717

[30] S. Ghotekar, D. Sanap, K.-Y. A. Lin, H. Louis, D. Pore, and R. Oza, "A novel green synthesis of honey-mediated CoCr2O4 nanoparticles and their expeditious heterogeneous catalytic role for the synthesis of 5-aryl-[1,2,4] triazolidine-3-thiones," Research on Chemical Intermediates, vol. 50, no. 1, pp. 49-68, Jan. 2024, doi: 10.1007/s11164-023-05155-8. https://doi.org/10.1007/s11164-023-05155-8

[31] D. Chaibeddra et al., "Synthesis, physical and electrochemical characterization of CoCr2O4 and its application as photocatalyst under solar irradiation," Inorg Chem Commun, vol. 155, p. 111116, Sep. 2023, doi: 10.1016/j.inoche.2023.111116. https://doi.org/10.1016/j.inoche.2023.111116

[32] P. K. Ngoc et al., "Superior organic dye removal by CoCr2O4 nanoparticles: Adsorption kinetics and isotherm," Journal of Science: Advanced Materials and Devices, vol. 7, no. 2, p. 100438, Jun. 2022, doi: 10.1016/j.jsamd.2022.100438. https://doi.org/10.1016/j.jsamd.2022.100438

[33] E. Konuk, "A meta-analysis assessing the cytotoxicity of nanoparticles on MCF7 breast cancer cells," Oncol Lett, vol. 28, no. 5, p. 551, Sep. 2024, doi: 10.3892/ol.2024.14684. https://doi.org/10.3892/ol.2024.14684

[34] D. Asmat-Campos, M. Lindsay Rojas, and A. Carreño-Ortega, "Toward sustainable nanomaterials: An innovative ecological approach for biogenic synthesis of TiO2 nanoparticles with potential photocatalytic activity," Clean Eng Technol, vol. 17, p. 100702, Dec. 2023, doi: 10.1016/J.CLET.2023.100702. https://doi.org/10.1016/j.clet.2023.100702

[35] R. an Doong and W. huei Chang, "Photodegradation of parathion in aqueous titanium dioxide and zero valent iron solutions in the presence of hydrogen peroxide," J Photochem Photobiol A Chem, vol. 116, no. 3, pp. 221-228, Jul. 1998, doi: 10.1016/S1010-6030(98)00292-5. https://doi.org/10.1016/S1010-6030(98)00292-5

[36] A. O. Oluwole and O. S. Olatunji, "Photocatalytic degradation of tetracycline in aqueous systems under visible light irridiation using needle-like SnO2 nanoparticles anchored on exfoliated g-C3N4," Environ Sci Eur, vol. 34, no. 1, p. 5, Dec. 2022, doi: 10.1186/s12302-021-00588-7. https://doi.org/10.1186/s12302-021-00588-7

[37] R. Aali et al., "Enhanced sulfadiazine degradation through synergistic visible light assisted peroxymonosulfate activation using a magnetic Fe_3O_4-$ZnIn_2S_4$ catalyst," Sci Rep, vol. 15, no. 1, p. 25013, Jul. 2025, doi: 10.1038/s41598-025-10973-4. https://doi.org/10.1038/s41598-025-10973-4

[38] M. Hasham Firooz, A. Naderi, M. Moradi, and R. R. Kalantary, "Enhanced tetracycline degradation with TiO2/natural pyrite S-scheme photocatalyst," Sci Rep, vol. 14, no. 1, p. 4954, Feb. 2024, doi: 10.1038/s41598-024-54549-0. https://doi.org/10.1038/s41598-024-54549-0

[39] A. H. Zyoud, "Photodegradation of aqueous tetracycline using CuS@TiO_2 composite under solar-simulated light: Complete mineralization, catalyst efficiency, and reusability," Heliyon, vol. 11, no. 2, p. e41662, Jan. 2025, doi: 10.1016/J.HELIYON.2025.E41662. https://doi.org/10.1016/j.heliyon.2025.e41662

[40] J. Wang, M. Zhu, A. Sun, R. Yuan, H. Chen, and B. Zhou, "The Influence Mechanism of Dissolved Organic Matter on the Photocatalytic Oxidation of Pharmaceuticals and Personal Care Products," Molecules, vol. 30, no. 11, p. 2266, May 2025, doi: 10.3390/molecules30112266. https://doi.org/10.3390/molecules30112266

[41] D. A. Kader, A. H. Mohammed, S. J. Mohammed, and D. M.

Aziz, "Transforming henna: from natural dye to photosensitizer for efficient photocatalytic degradation of 4-nitrophenol using a green-synthesized ZnO@henna nanocomposite," RSC Adv, vol. 15, no. 23, pp. 18245-18265, 2025, doi: 10.1039/D5RA02154E. https://doi.org/10.1039/D5RA02154E

[42] D. A. Bopape, B. Ntsendwana, and F. D. Mabasa, "Photocatalysis as a pre-discharge treatment to improve the effect of textile dyes on human health: A critical review," Heliyon, vol. 10, no. 20, p. e39316, Oct. 2024, doi: 10.1016/J.HELIYON.2024.E39316. https://doi.org/10.1016/j.heliyon.2024.e39316

[43] K. Patel et al., "Insights into the solar-light-driven photocatalysis of greenly synthesized CoCr2O4 nanoparticles using Azadirachta indica," J Solgel Sci Technol, vol. 114, no. 2, pp. 594-611, May 2025, doi: 10.1007/s10971-025-06711-x. https://doi.org/10.1007/s10971-025-06711-x

[44] D. Chaibeddra et al., "Synthesis, physical and electrochemical characterization of CoCr2O4 and its application as photocatalyst under solar irradiation," Inorg Chem Commun, vol. 155, p. 111116, Sep. 2023, doi: 10.1016/j.inoche.2023.111116. https://doi.org/10.1016/j.inoche.2023.111116

[45] 3, RezaFoorotan1, FarzanehMoradnia1, ZolfaAfshari1 andAliRamazani SaeidTaghaviFardood1, "Greensynthesis, characterization, and photocatalytic activity of cobalt chromite spinel nanoparticles," Material Research Express, vol. 7, 2020. https://doi.org/10.1088/2053-1591/ab6c8d

[46] K. Ghorai et al., "Facile synthesis of CuCr2O4/BiOBr nanocomposite and its photocatalytic activity towards RhB and tetracycline hydrochloride degradation under household visible LED light irradiation," J Alloys Compd, vol. 867, p. 157947, Jun. 2021, doi: 10.1016/j.jallcom.2020.157947. https://doi.org/10.1016/j.jallcom.2020.157947

[47] K. Michalec, B. Mozgawa, A. Kusior, P. Pietrzyk, Z. Sojka, and M. Radecka, "Tunable Generation of Reactive Oxygen Species in SnO 2 /SnS 2 Nanostructures: Mechanistic Insights into Indigo Carmine Photodegradation," The Journal of Physical Chemistry C, vol. 128, no. 12, pp. 5011-5029, Mar. 2024, doi: 10.1021/acs.jpcc.3c08165. https://doi.org/10.1021/acs.jpcc.3c08165

[48] M. S. Athar, Z. Rasool, M. Muneer, H. M. Altass, I. I. Althagafi, and S. A. Ahmed, "Fabrication of Direct Z-Scheme CoNiWO 4 / Ph-gC 3 N 4 Heterocomposites: Enhanced Photodegradation of Bisphenol A and Anticancer Activity," ACS Omega, vol. 8, no. 41, pp. 38272-38287, Oct. 2023, doi: 10.1021/acsomega.3c04653. https://doi.org/10.1021/acsomega.3c04653

[49] C. Yu et al., "Visible-light-enhanced photocatalytic activity of BaTiO3/γ-Al2O3 composite photocatalysts for photodegradation of tetracycline hydrochloride," Opt Mater (Amst), vol. 135, p. 113364, Jan. 2023, doi: 10.1016/j.optmat.2022.113364. https://doi.org/10.1016/j.optmat.2022.113364

[50] S. Gaffar, A. Kumar, J. Alam, and U. Riaz, "Efficient visible light-induced photocatalytic degradation of tetracycline hydrochloride using CuFe2O4 and PANI/CuFe2O4 nanohybrids," Environmental Science and Pollution Research, vol. 30, no. 50, pp. 108878-108888, Sep. 2023, doi: 10.1007/s11356-023-29976-7. https://doi.org/10.1007/s11356-023-29976-7

[51] K. Hemavibool, T. Sansenya, and S. Nanan, "Enhanced Photocatalytic Degradation of Tetracycline and Oxytetracycline Antibiotics by BiVO4 Photocatalyst under Visible Light and Solar Light Irradiation," Antibiotics, vol. 11, no. 6, p. 761, Jun. 2022, doi: 10.3390/antibiotics11060761. https://doi.org/10.3390/antibiotics11060761

[52] S. Singh, S. Parveen, L. Clarizia, and P. Kumar, "An insight into photo-catalytic degradation mechanism of persistent pollutants with transition metal oxides and their composites: Photocatalysis mechanism, rate affecting parameters, and removal pathways," Catalysis Reviews, pp. 1-49, Jan. 2025, doi: 10.1080/01614940.2024.2440664. https://doi.org/10.1080/01614940.2024.2440664